Transport entropy in $YBa_2Cu_3O_7$: A comparison between epitaxial and polycrystalline thin films

F. Kober, H.-C. Ri, R. Gross, D. Koelle, and R. P. Huebener
Physikalisches Institut, Lehrstuhl Experimentalphysik II, Universität Tübingen, D-7400 Tübingen, Federal Republic of Germany

A. Gupta
IBM Research Division, Thomas J. Watson Research Center, Yorktown Heights, New York, 10598
(Received 8 April 1991)

The dissipative behavior in thin films of $YBa_2Cu_3O_{7-\delta}$ has been investigated under the influence of a temperature gradient. By using the sample configuration itself as a thermometer, a method has been developed for the study of flux dynamics in the presence of a temperature gradient. The temperature and magnetic-field dependence of the transport entropy was measured, and the influence of grain boundaries on this quantity was investigated. For an epitaxial $YBa_2Cu_3O_{7-\delta}$ film near T_c, we obtain the value $-dH_{c2}/dT=2\pm0.5$ T/K and the Ginzburg-Landau parameter $\kappa_{GL}=80\pm10$.

I. INTRODUCTION

Since the discovery of the high-temperature superconductors, much research has been done to understand the resistive transition to the superconducting state and the dissipative behavior in the mixed state of these materials. With the vortex-pinning energies of the high-temperature superconductors being comparable to thermal energies in a large part of the magnetic-field–temperature (H-T) phase space, the dissipation in this regime appears to be dominated by thermally assisted flux motion.[1,2] This process has been successfully described by diffusion models.[3,5] While some researchers have shown that the broadening of the resistive transition due to an external magnetic field can be understood within a flux-creep model, sensitive transport measurements have shown that the current-voltage characteristics[6] exhibit a power-law behavior favoring a model based on a phase transition from a vortex glass to a vortex liquid.[7] Furthermore, the large anisotropy of the high-T_c materials leads to an intrinsic quasi-two-dimensional (2D) behavior associated with the single CuO_2 planes. Therefore, the behavior of the high-T_c materials may be described in terms of Kosterlitz-Thouless theory[8,9] also in the case of bulk materials. Recently, this concept has been extended to the case of external magnetic fields including coupling between the CuO_2 planes.[10]

Up to now, most experiments studying the dissipative behavior in the mixed state of the high-temperature superconductors are usual transport or magnetization measurements involving only the Lorentz force as the driving force. During the last year, a number of groups have investigated the dynamics of the flux lines also under the influence of a temperature gradient, resulting in a thermal driving force. Zeh *et al.* have observed the Nernst effect in polycrystalline[11] and epitaxial[12] thin films of $YBa_2Cu_3O_{7-\delta}$. Further experimental evidence for the Nernst effect in polycrystalline Bi-Sr-Ca-Cu-O samples has been given by Galffy, Freimuth, and Murek[13] and in Tl-Ba-Ca-Cu-O thin films by Lengfellner *et al.*[14] While the results obtained by these groups had more or less qualitative character, Palstra *et al.*[15] reported quantitative results for the temperature dependence of the transport energy per flux line, U_Φ, by measuring the Ettingshausen effect in a $YBa_2Cu_3O_{7-\delta}$ single crystal. Using the theory of Werthammer, Helfand, and Hohenberg,[16] they derived a value of $-dH_{c2}/dT$ and $\xi_{ab}(0)$ from their experimental data. Motivated by these data, Ullah and Dorsey[17] calculated $U_\Phi(T)$ at temperatures above T_c within the model of critical fluctuations. Recently, Hagen *et al.*[18] presented quantitative results on the transport entropy versus temperature in epitaxial thin films of $YBa_2Cu_3O_{7-\delta}$ based on the Nernst effect. Although their results for $U_\Phi(T)$ are in good agreement with the data of Palstra *et al.*, they differ by a factor of 4 from those obtained from magnetization measurements.[19,20]

In order to clarify the reason for the different experimental observations and to obtain experimental information on dH_{c2}/dT for a thin-film sample, we have performed a detailed study of the Nernst effect in both epitaxial and polycrystalline $YBa_2Cu_3O_{7-\delta}$ films. The temperature and magnetic-field dependence of the electric resistivity, Nernst coefficient, and, hence, transport entropy has been measured. A new experimental method has been developed to control and measure both the value of the temperature gradient *and* the temperature in the film with high accuracy. Furthermore, a well-characterized, polycrystalline sample has been studied in order to demonstrate the effect of grain boundaries or, in general, other resistive mechanisms on the derived value of the transport entropy. The significance of the experimental value of U_Φ in different temperature regimes will be discussed and compared with other reported results.

II. BASIC EQUATIONS

From measurements of the Nernst effect, one can obtain the temperature dependence of the transport entropy of a flux line, $S_\Phi(T)$, which yields information on the

coherence length ξ of the high-T_c superconductor. If a temperature gradient $\nabla_x T$ is applied to a superconducting sample in the x direction in the presence of a magnetic field B_z in the z direction, the vortices experience the thermal force $F_{\rm th}=-S_\Phi \nabla_x T$, pointing from the hot to the cold end of the sample and generating a transverse electric field $E_y^{\rm th}$ in the y direction.[21] In the stationary state, the flux lines move at a constant velocity $v_x^{\rm FL}$, which is determined by the balance of the thermal and damping forces:

$$-S_\Phi \nabla_x T-\eta v_x^{\rm FL}=0 \ . \tag{1}$$

Here η is the damping coefficient. In Eq. (1) and in the following, all forces are taken per unit length of flux lines by defining the relevant quantities accordingly. Further, we assume that the concept of thermally activated flux diffusion applies because of the small magnitude of the driving force (in this case the flux-pinning force does not appear explicitly). Note that in a thermal force measurement we can measure only $\nabla_x T$ and $v_x^{\rm FL}=E_y^{\rm th}/B$. Therefore, in order to obtain S_Φ, the coefficient η has to be measured independently. The latter can be done by a usual transport measurement, applying the Lorentz force as the driving force. In this case the balance of forces is given by

$$+j_y \Phi_0-\eta v_x^{\rm FL}=0 \ . \tag{2}$$

Here Φ_0 is the magnetic-flux quantum. The quantities j_y and $v_x^{\rm FL}=E_y^L/B$ can be measured, and hence η is obtained directly. Here $E_y^L=\rho j_y$ is the electric field generated by the vortex motion; ρ is the corresponding resistivity. Because of the anisotropy of the high-T_c materials, in the combination of Eqs. (1) and (2) the Lorentz force F_L must act in the same direction as the thermal force. Keeping this in mind, the value of $\eta=(\Phi_0 B)/\rho$ determined from Eq. (2) can be inserted into Eq. (1) and we obtain

$$S_\Phi=\frac{\Phi_0 E_y^{\rm th}}{\rho \nabla_x T} \ . \tag{3}$$

The following theoretical expression for $S_\Phi(T)$ has been derived by Maki[22] from the time-dependent Ginzburg-Landau theory:

$$S_\Phi=\frac{\Phi_0}{4\pi T}\frac{[H_{c2}(T)-H]}{1.16(2\kappa_{\rm GL}^2-1)+1}L_D(T) \tag{4a}$$

$$=\frac{\Phi_0}{T}\langle M\rangle L_D(T) \ . \tag{4b}$$

Here $\langle M\rangle$ is the spatially averaged magnetization in the sample, $\kappa_{\rm GL}$ is the Ginzburg-Landau parameter, and $L_D(T)$ is a numerical function close to 1 near T_c. The arguments by Maki have been corrected subsequently by Hu.[23] The transport energy per unit length of a flux line is defined as

$$U_\Phi=TS_\Phi \ . \tag{5}$$

At temperatures close to T_c, Ginzburg-Landau theory yields $dH_{c2}/dT=$const. Hence dU_Φ/dT is expected to be constant if the temperature dependence of L_D is negligible.

It is important to note that Eq. (3) holds as long as the following conditions are fulfilled.

(1) The damping coefficient η is the same for the application of the thermal force and the Lorentz force.

(2) The coefficient η does not depend on j_y or $\nabla_x T$; i.e., the $E_y(\nabla_x T)$ and $E_y(j_y)$ relations are assumed to be linear.

If these conditions are not fulfilled, the calculation of S_Φ according to Eq. (3) does not yield the correct result. To illustrate that point, we consider the following example. Let us assume that the total resistivity ρ measured in the electric transport measurement is given by the series connection of two components $\rho_{\rm FF}$ and ρ_R, i.e., $\rho=\rho_{\rm FF}+\rho_R$. Here the component $\rho_{\rm FF}$ is caused by the motion of Abrikosov vortices and ρ_R is caused by other resistive mechanisms. Because of the finite value of ρ_R, we have $\rho>\rho_{\rm FF}$ and hence the derived damping coefficient $\eta=\Phi_0 B/\rho$ becomes smaller than the true value $\eta^*=\Phi_0 B/\rho_{\rm FF}$. This results in a reduced value of the apparent transport entropy:

$$S_\Phi(\rho)=S_\Phi(\rho_{\rm FF})\frac{\rho_{\rm FF}}{\rho_{\rm FF}+\rho_R} \ . \tag{6}$$

Equation (6) demonstrates that any resistive mechanism, which is not related to Abrikosov vortex motion but contributes to the electric transport measurement, results in a reduced value of S_Φ. There may be different reasons for an additional resistive mechanism ρ_R contributing to ρ, as indicated by the following examples.

(i) A part of the sample is normal conducting.

(ii) The sample contains grain boundaries. The resistivity due to these grain boundaries is associated with the motion of Josephson vortices along them. Note that Josephson vortices do not contribute to the Nernst voltage, since they do not transport entropy as a result of the absence of a normal core.

(iii) The sample represents a quasi-two-dimensional (2D) system. Because of the two dimensionality, there is a finite probability for the generation of thermally activated vortex-antivortex (V-AV) pairs.[9] In the presence of V-AV pairs, the response of the sample is different in a Lorentz force and a thermal force experiment. In the case of a Lorentz force, the unbinding of the pairs results in a finite voltage, since the vortex and antivortex move in opposite directions. In contrast, if a thermal force is applied, both the vortex and antivortex are driven in the same direction, since the transport entropy does not depend on the sign of the magnetic field. In this case the time-averaged voltage is zero.

III. EXPERIMENTAL TECHNIQUE

In order to establish a temperature gradient in the thin-film samples, we have developed a sample holder described in detail in Ref. 11. The substrate is mounted in the x-y plane between two gold-plated copper blocks, which are thermally decoupled. The temperature of each copper block can be controlled separately with an accura-

cy of better than 5 mK. The whole arrangement is surrounded by a stainless-steel vacuum can. The sample holder is inserted into liquid He and centered in a superconducting magnet, generating fields up to 4 T in the z direction. Setting the two copper blocks to different temperatures T_1 and T_2, respectively, a temperature gradient $\nabla_x T$ is maintained in the x direction. The transverse electric field E_y, generated by the moving flux lines, is always measured for the two opposite directions of the magnetic field in order to eliminate any other contributions (such as a thermoelectric voltage in the voltage leads).

The mean value of the sample temperature and temperature gradient must be known with high accuracy. The temperature gradient in the film is determined by the heat current I^h through the substrate and its thermal conductivity κ. Here the contribution of the superconducting film can be neglected, since the thickness of the substrate is 1000 times larger than that of the film. I^h is given by the temperature difference $\Delta T = T_1 - T_2$ between the copper blocks and total heat resistance between them, which, in turn, is given by the sum of the heat resistance of the substrate and thermal boundary resistance between the substrate and copper blocks. The thermal coupling between the substrate and copper blocks is established by gluing the bottom of the substrate with stycast to the copper blocks. However, the thermal boundary resistance cannot be neglected and may vary from sample to sample. Therefore, it is necessary to measure $\nabla_x T$ in the substrate directly. In principle, we can proceed with a differential thermocouple, fixed on the surface of the substrate somewhere between the copper blocks. However, this procedure has two disadvantages: First, the resolution in measuring the value of $\nabla_x T$ is limited by the spatial extension of the thermocouple contacts and distance between them. Second, while the value of $\nabla_x T$ can be measured in this way, the absolute value of the temperature at a fixed location x on the substrate cannot be determined. Consequently, the thermocouple technique appears inconvenient for recording temperature-gradient-dependent data at constant sample temperature

Therefore, we have developed a special procedure, which enables us to measure both $\nabla_x T$ and the absolute temperature at a location x in the film with high accuracy. Here the key feature is the use of the superconducting thin film itself as the thermometer. This requires a special sample geometry shown in Fig. 1. Two parallel strips A and B oriented perpendicular to $\nabla_x T$ are crossed by strip C, which runs along the x direction. Strip C is only used to measure the thermopower, as has been reported elsewhere.[24] While all data concerning the Nernst effect are taken from strip A, both strips A and B are used for the temperature calibration of the system. Our procedure is as follows: First, with $\Delta T = 0$ the temperature dependence of the resistivity of both strips, $\rho_A(T)$ and $\rho_B(T)$, is measured. Then the two copper blocks are set to different temperatures, i.e., $T_1 \neq T_2$, and ρ_A and ρ_B are measured in this stationary state. With these values and the "calibration curves" $\rho_A(T)$ and ρ_B, we obtain $T(A)$ and $T(B)$, respectively, i.e., the temperatures of strips A and B for $T_1 \neq T_2$. Repeating the last step for different values of ΔT, keeping $T_M = (T_1 + T_2)/2$ constant, we obtain the typical curves plotted in Fig. 2. From the slope of the lines, we find the numerical factors $F_1 = [T(A) - T(B)]/(T_1 - T_2)$ and $F_2 = [T_1 - T(A)]/(T_1 - T_2)$. (We have performed this procedure at various temperatures T_M using a specimen with a very broad resistive transition and found a variation of the factors F_1 and F_2 less than 1% up to $\Delta T_M = 5$ K.) Finally, the value of $\nabla_x T$ is given by

$$\nabla_x T = (T_2 - T_1) F_1 / d \ . \tag{7}$$

Here d is the distance between strips A and B ($d = 3$ mm). In the same way the temperature of strip A can be calculated from T_1 and T_2 using

$$T(A) = T_1 + F_2 (T_2 - T_1) \ . \tag{8}$$

Since the Nernst voltage depends on $\nabla_x T$ only (in contrast to the Seebeck effect, where the voltage signal scales with the absolute-temperature difference between the contacts), the width W in the x direction of strips A and B was only about 100 μm. Hence, with an applied temperature gradient up to $\nabla_x T = 10$ K/cm, the temperature difference between the hot and cold ends of the strip does not exceed 100 mK. In this way high accuracy for the sample temperature is obtained. The length L of strips A and B was 8 mm, again for obtaining large resolution in the $E_y/\nabla_x T$ data. This length was only limited by the size of the substrate.

In order to examine the accuracy of the control of the thermal parameters in our experimental arrangement, we have measured $E_y(\nabla_x T)$ of strip A of a polycrystalline sample (see Sec. V) at $B = 4$ T and constant temperature, as shown in Fig. 3. This has been done for the two opposite directions of magnetic field by slowly sweeping the temperatures of the two copper blocks in opposite directions, such that the temperature at the position of strip A remained constant. Then the electric resistivity was measured under the same thermal conditions, and the result is shown in the upper curve of Fig. 3. Knowing $d\rho/dT$ (see the inset of Fig. 3), the mean temperature in the strip was found to stay constant with about 30 mK at $T = 77.1$ K during the variation of $\nabla_x T$ from -20 to $+10$ K/cm.

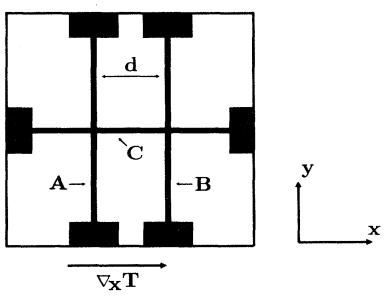

FIG. 1. Schematic diagram of the Y-Ba-Cu-O sample film on the $SrTiO_3$ substrate. Strips A and B are used to perform the temperature calibration of the system. The Nernst coefficient and resistivity have been measured with strip A.

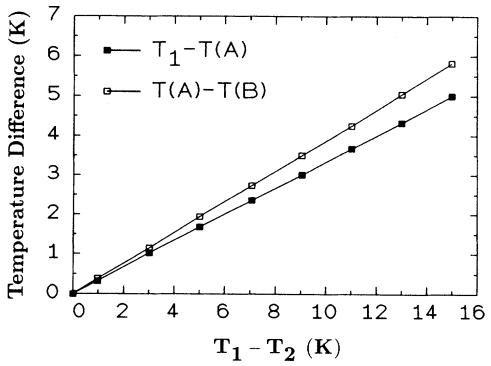

FIG. 2. Temperature calibration with the epitaxial film. $T1$-$T(A)$: Difference between the temperature of one copper block, $T1$, and the temperature of strip A, $T(A)$. $T(A)$-$T(B)$: Difference between the temperatures of the strips A and B. $T1$-$T2$: Difference between the temperatures of the two copper blocks. With the slopes of these lines, the temperature and temperature gradient at the location of strip A can be calculated from the measured temperatures in the copper blocks, $T1$ and $T2$.

This demonstrates the capability of our system to vary $\nabla_x T$ considerably while keeping the sample temperature constant. [This, for example, is important for checking the linearity of the $E_y(\nabla_x T)$ dependence.] Taking $dE_y/d(\nabla_x T)$ from Fig. 3 and using Eqs. (3) and (5) yields $U_\Phi(77.1\ \mathrm{K}) = 3.33 \times 10^{-14}$ J/m. In Sec. V we will return to this result.

IV. EPITAXIAL FILM; EXPERIMENTAL RESULTS AND DISCUSSION

In the following we show data obtained with an epitaxial, c-axis-oriented thin film of $YBa_2Cu_3O_{7-\delta}$ on (100) $SrTiO_3$ prepared by laser ablation deposition.[25] The film was 200 nm thick and was patterned by photolithography and wet etching. The critical current density was 2×10^6 A/cm^2 at 77 K. In Fig. 4(a) the electric resistivity of strip A is plotted versus temperature for different magnetic fields parallel to the c axis ($B = 0$–4 T). The value of $\rho(100\ \mathrm{K}) = 60\ \mu\Omega$ cm agrees with earlier results reported for similar laser-ablated films.[26,27] The broadening of the resistive transition due to the applied magnetic field shows the typical behavior obtained for epitaxial Y-Ba-Cu-O.[2]

Figure 4(b) shows the temperature dependence of the Nernst coefficient $E_y/\nabla_x T$ of the same strip for magnetic fields from 1 to 4 T. The data points were measured in the stationary state at an applied temperature gradient of 13 K/cm. Their resolution was better than 5 nV/K. The

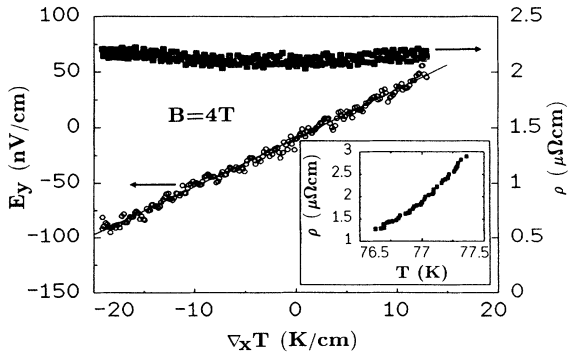

FIG. 3. Polycrystalline sample: Resistivity (upper curve) and Nernst electric field (lower curve) vs temperature gradient of strip A at $B = 4$ T. Inset: Resistivity vs temperature. Combining the upper and $\rho(T)$ curves, it is confirmed that the temperature of the strip was constant at $T = 77.1 \pm 0.03$ K, during the variation of $\nabla_x T$ from -20 to $+10$ K/cm.

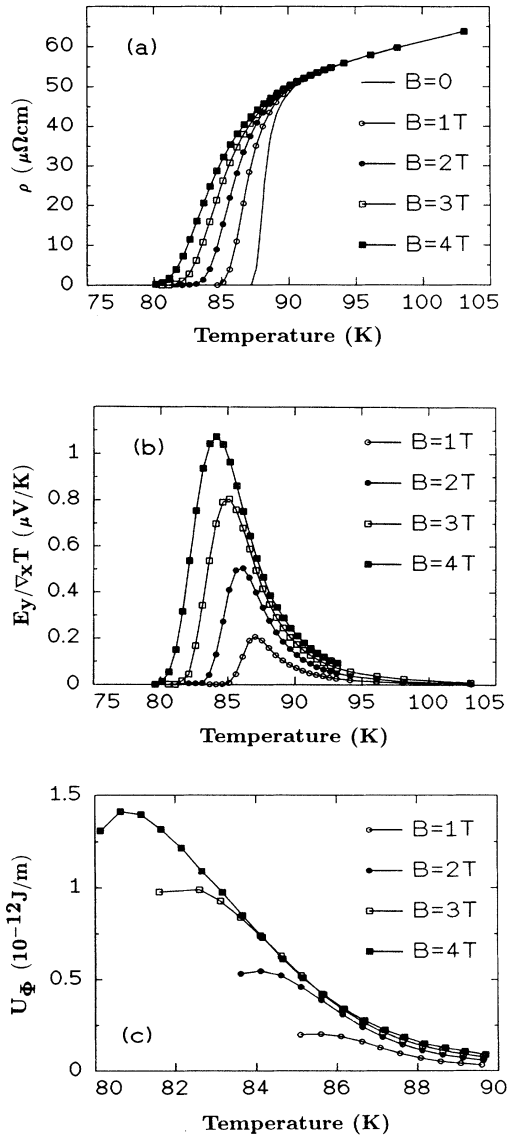

FIG. 4. Epitaxial film data. (a) Resistivity vs temperature of strip A for magnetic fields perpendicular to the film plane (**B**| |**c**) from 0 to 4 T. (b) Nernst coefficient vs temperature for the same strip and same magnetic fields. (c) Temperature dependence of the transport energy per unit length of flux line U_Φ calculated from the data shown in (a) and (b) using Eqs. (3) and (5). Note the different temperature scale.

lines are only for guiding the eye. As expected, a nonvanishing Nernst coefficient is observed mainly in the temperature range where the resistivity is caused by flux motion. At lower temperatures the signal becomes unmeasurably small as a result of the increasing flux-pinning strength. Above T_c there is a large tail, which may be understood in terms of fluctuation effects, as will be discussed below. The absolute magnitude of the Nernst coefficient reflects the product between the resistivity and transport entropy of the sample [see Eq. (3)]. From the measured data we have calculated $U_\Phi(T)$ using Eqs. (3) and (5). For this we have inserted the measured resistivity $\rho(B,T)$ of the strip up to $T=90$ K shown in Fig. 4(a). The result is shown in Fig. 4(c), where $U_\Phi(T)$ is plotted as a function of temperature for the different magnetic fields. The expected behavior discussed in Sec. II is clearly observed. At $T=81$ K, $\nabla_x T=13$ K/cm, and $B=4$ T, the thermal force per unit length of the flux line, is about 2.2×10^{-11} J/cm^2, corresponding to the Lorentz force of a current density of ~1.1 A/cm^2. However, $j_y=5$ A/cm^2 was used to measure the resistivity. To see whether this difference in the magnitude of the thermal and Lorentz forces affects the results of Fig. 4(c), we have measured both the $E_y(\nabla_x T)$ and $E_y(j_y)$ dependence at different temperatures. In agreement with the expected thermally activated nature of flux motion in our sample, in both cases a linear proportionality was found.

Extrapolating the linear parts of $U_\Phi(T)$ linearly to zero, we obtain $T_c(H)$ and, hence, $H_{c2}(T)$. From this we find the value $dH_{c2}(T)/dT=-2\pm0.5$ T/K. The large error is caused by the small extent of the linear range of $U_\Phi(T)$ at low fields. In this calculation the temperature dependence of the numerical function $L_D(T)$ has been neglected. According to the $L_D(T)$ curve shown in Ref. 22, in the present case the contribution of dL_D/dT to the value of dU_Φ/dT is less than 10% at $T=0.9T_c$ and becomes even smaller with T approaching T_c.

In order to compare the results of the different experiments reported so far, it is reasonable to use the derivative dU_Φ/dT at a fixed value of magnetic field, since U_Φ exhibits a strong temperature dependence near T_c and different samples usually show different T_c values. In Table I we have listed dU_Φ/dT ($B=3$ T) from Hagen *et al.* (Nernst effect),[18] Palstra *et al.* (Ettingshausen effect),[15] and Hao *et al.* (magnetization measurements),[20] in addition to our own results. Hao *et al.* measured the magnetization $\langle M\rangle$ of a single crystal, from which we have calculated dU_Φ/dT using Eqs. (4b) and (5) with $L_D(T)=1$ near T_C. There is good agreement between our data on dH_{c2}/dT and those of Hao *et al.*, which, in turn, agree with earlier magnetization measurements.[19] Since both dU_Φ/dT and dH_{c2}/dT are measured quantities, we can calculate the Ginzburg-Landau parameter κ_{GL} using

$$\kappa_{GL}\left[\frac{\Phi_0}{9.28\pi}\frac{dH_{c2}}{dT}\Big/\frac{dU_\Phi}{dT}\right]^{1/2}, \tag{9}$$

which is a good approximation in the case of $\kappa_{GL}\gg1$. The result is included in Table I. We note that both dU_Φ/dT and $-dH_{c2}/dT$ obtained from our measurements are smaller by a factor of 3 than the values reported by Palstra *et al.*[15] However, κ_{GL} is nearly the same.

The high value of dU_Φ/dT reported by Hagen *et al.* appears to be affected by their geometric configuration. The authors used a thin film with an extension d of only 50 μm perpendicular to the temperature gradient, whereas the length of their sample parallel to the temperature gradient was relatively long. The electrical connections to the film were provided by 50-μm Au wires. Since $E_y=V_y/d$ is needed to calculate U_Φ, the accuracy of d determines the error in the value of U_Φ. This error can be reduced considerably by using a sample configuration such as shown in Fig. 1.

V. POLYCRYSTALLINE FILM; EXPERIMENTAL RESULTS AND DISCUSSION

An important problem associated with high-T_c superconducting thin-film samples is the existence of extended defects or inhomogeneities present also in "high quality" epitaxial films.[28] Since the $U_\Phi(T)$ characteristics of the epitaxial film shown in Fig. 4(c) clearly deviate from the expected linearity both in the limit of low and high temperatures, the influence of inhomogeneities on the measured value of the transport entropy has to be clarified.

TABLE I. Comparison of the results of different groups for the temperature derivative of the transport line energy, dU_Φ/dT, the temperature dependence of the upper critical field, dH_{c2}/dT, and the Ginzburg-Landau parameter κ_{GL} near T_c. The results were obtained using different experimental techniques: Hagen *et al.* (Nernst effect in a thin film), (Ref. 18) Palstra *et al.* (Ettingshausen effect in a single crystal), (Ref. 15) Hao *et al.* (magnetization in a single crystal) (Ref. 20).

	Sample type	$-dU_\Phi/dT(B=3$ T) (J/K m)	$-dH_{c2}/dT$ (T/K)	κ_{GL}
Present results	thin film	2.2×10^{-13}	2±0.5	80±10
Palstra *et al.*[a]	single crystal	6.6×10^{-13}	7±1	86±6
Hagen *et al.*[b]	thin film	8.8×10^{-13}		
Hao *et al.*[c]	single crystal	4.0×10^{-13}	1.65±0.23	54±4

[a]See Ref. 15.
[b]See Ref. 18.
[c]See Ref. 20.

For that reason we have investigated a polycrystalline $YBa_2Cu_3O_{7-\delta}$ film prepared by dc-magnetron sputtering on (100) $SrTiO_3$. The substrate temperature during the sputtering process was kept at 680 °C, resulting in a critical temperature of 82.5 K. X-ray-diffraction analysis showed a high portion of a-axis-oriented ($\geq 90\%$) and a small portion of c-axis-oriented ($\leq 10\%$) film areas. The a-axis lattice constant derived from these x-ray data indicated a high oxygen content ($\delta \leq 0.02$). The $\rho(T)$ characteristic has been measured before and after the patterning process (wet etching), and no change could be detected. The sample geometry was the same as that of the epitaxial film (Fig. 1). The critical current density j_c of strip A was 2×10^4 A/cm^2 at 77 K and 1.6×10^5 A/cm^2 at 70 K (using the criterion $E_y = 1$ μV/cm). The film was 240 nm thick and the surface was smooth; no structure was observed by reflection-electron-microscopy (REM) measurements with a resolution of 30 nm.

The structural characterization of the sample shows that it consists of mostly a-axis-oriented grains. Of course, the a-axis-oriented material may have different orientations of the c axis. Therefore, for measurements with $\mathbf{B} \| \mathbf{a}$, the absolute magnitude of the transport entropy represents a value spatially averaged over the different directions of vortex motion relative to the c axis. However, the temperature and magnetic-field dependences of S_Φ give information on the effect of the grain boundaries present in the film.

This section is organized as follows: in Sec. V A the temperature-dependent experimental data are shown. In Secs. V B–V D the results obtained for $U_\Phi(T)$ will be discussed in the different temperature regimes $T > T_{c0}(B=0)$ (Sec. V B), $T_{c0}(B) < T < T_{c0}(B=0)$ (Sec. V C), and T near $T_{c0}(B)$ (Sec. V D).

A. Experimental results: temperature dependence

In Fig. 5(a) the resistivity of strip A is shown for $B=0$ and 4 T. The temperatures, where the resistivity falls below the resolution limit, are $T_{c0}(B=0) \approx 82.5$ K and $T_{c0}(B=4\text{ T}) \approx 77$ K. The spread of the T_{c0} values due to the magnetic field is less than that observed for c-axis-oriented material, but somewhat larger than that of a completely a-axis-oriented material.[2] This is in agreement with the film composition. In Fig. 5(b), $E_y/\nabla_x T$ of the same strip is plotted versus temperature for different magnetic fields. Here T_1 and T_2 have been varied continuously, keeping $T_1 - T_2 = 10$ K constant. The accuracy of the absolute-temperature measurement was 30 mK, and the voltage resolution was better than 3 nV/K. The curves exhibit broader peaks compared to the epitaxial film, corresponding to the larger temperature width of the resistive transition. However, their maxima appear at almost the same temperatures as those in Fig. 4(b). We note that at $T=96$ K the Nernst coefficient is about the same as that of the epitaxial film, whereas its maximum value at $T=85$ K is about 5 times smaller. In order to show the important features, we focus on the 4-T data. Figure 5(c) shows the $U_\Phi(T)$ dependence as $B=4$ T, as calculated from the measured data using Eqs. (3) and (5). Beyond the expected linear decrease of $U_\Phi(T)$ for $T_{c0}(4\text{ T}) < T < T_{c0}(0\text{ T})$, $U_\Phi(T)$ shows some unexpected behavior at $T < T_{c0}(4\text{ T})$ and for $T > T_{c0}(0\text{ T})$. In the following the $U_\Phi(T)$ dependence is discussed for these three different temperature regimes.

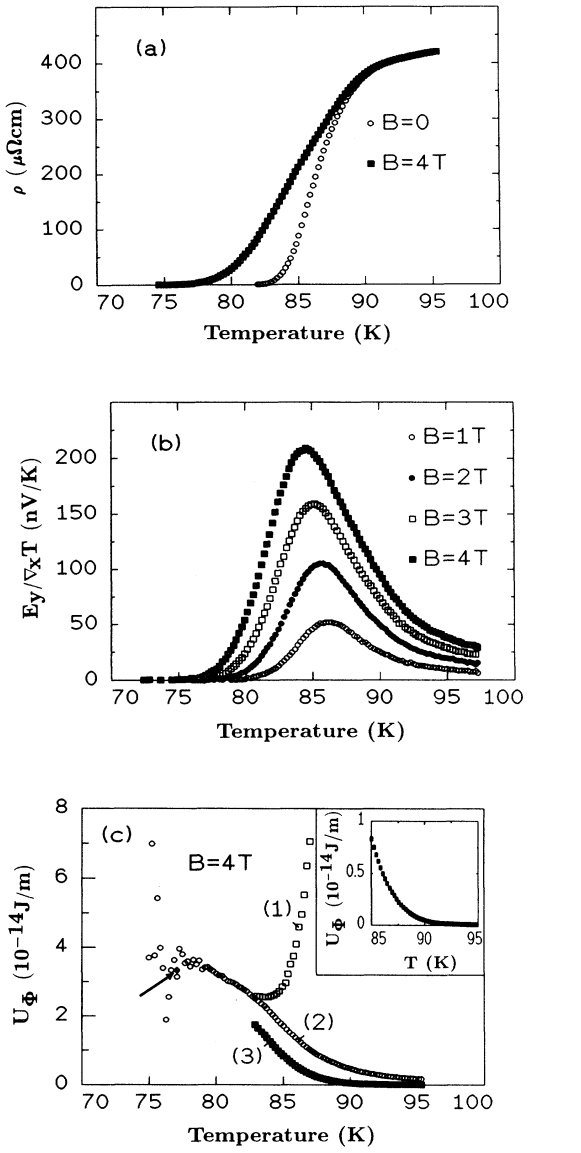

FIG. 5. Polycrystalline film data. (a) Resistivity vs temperature of strip A for $B=0$ and 4 T. Because of the 90% a-axis orientation of the film, $\mathbf{B} \| \mathbf{a}$ in most parts of the film. (b) Nernst coefficient vs temperature of the same strip for magnetic fields from 1 to 4 T. (c) Temperature dependence of the transport energy per unit length U_Φ calculated from the data of (a) and (b) using Eqs. (3) and (5). The three different branches above 83 K correspond to three different expressions for the resistivity used in this calculation. The data point indicated by the arrow is obtained from Fig. 3. Its error bars in U_Φ and T, respectively, are smaller than the size of the square. Inset: Curve 3 plotted with higher resolution.

B. $T > T_{c0}(B=0)$

As discussed in Sec. II, we have to use the resistivity $\rho_{FF}(T)$ caused by the motion of Abrikosov vortices for the calculation of $S_\Phi(T)$ and $U_\Phi(T)$. At $T > T_{c0}(B=0)$ the calculation of $U_\Phi(T)$ from the measured data is difficult, since it is not known which fraction of the measured resistivity is caused by moving flux lines carrying entropy. To demonstrate this difficulty, in Fig. 5(c) we have plotted $U_\Phi(T)$ using three different expressions for ρ_{FF}. Curve 1 in Fig. 5(c) is obtained by using

$$\rho(B,T)=\rho_{FF}(B,T)+\rho(B=0,T) . \tag{10}$$

Here we have assumed that the measured resistivity $\rho(B,T)$ is composed of two components connected in series, namely, a component due to flux motion, ρ_{FF}, and a second component equal to $\rho(B=0,T)$, not related to flux motion. The dramatic increase of $U_\Phi(T)$ suggests that the expression (10) for finding ρ_{FF} does not describe the true situation. Note that, according to Eq. (4), $U_\Phi(T)$ can only decrease with increasing temperature near T_c. Curve 2 in Fig. 5(c) was obtained using $\rho_{FF}(B,T)=\rho(B,T)$. That is, the measured resistivity $\rho(B,T)$ is assumed to be caused completely by flux motion, also at temperatures above the mean-field transition temperature T_c. Although the curve looks reasonable, it is doubtful that this describes the true situation. At least above T_c a major part of the measured resistivity should not be related to flux motion. Curve 3 in Fig. 5(c) is obtained by assuming

$$\frac{1}{\rho(B,T)}=\frac{1}{\rho_{FF}(B,T)}+\frac{1}{\rho_N(B,T)} . \tag{11}$$

Here we have assumed that $\rho(B,T)$ is composed of two components connected in parallel, namely, a component due to flux motion, ρ_{FF}, and a component due to normal conducting electrons, $\rho_N(B,T)$. Here $\rho_N(B,T)$ is extrapolated linearly from the higher-temperature regime down to temperatures below $T_c(B)$. It is evident from Eq. (11) that $\rho_{FF}(B,T)\to\rho(B,T)$ for T well below T_c, since here $\rho(B,T)\ll\rho_N(B,T)$. In contrast, for T well above T_c, $\rho(B,T)\to\rho_N(B,T)$ and, hence, $\rho_{FF}(B,T)\to\infty$. Note that Eq. (11) characterizes the situation where we have both superconducting and normal-conducting regions in the sample with the resistive mechanism in the superconducting regions described by ρ_{FF} and that in the normal-conducting regions by ρ_N. Of course, superconducting regions can exist also above T_c as a result of fluctuations, that is, ρ_{FF} remaining finite for $T > T_c$. Equation (11) seems to be a reasonable expression for the resistivity, at least for a high quality epitaxial film without any grain boundaries. In the presence of grain boundaries, Eq. (11) has to be modified to take into account the additional series resistivity ρ_{GB} caused by the grain boundaries resulting in $\rho(B,T)=(\rho_{FF}^{-1}+\rho_N^{-1})^{-1}+\rho_{GB}$.

In conclusion, Fig. 5(c) demonstrates that the result obtained for $U_\Phi(T)$ strongly depends on the expression used for $\rho_{FF}(T)$. However, the determination of ρ_{FF} by electric transport measurements is difficult. Therefore, a quantitative comparison of the experimental $U_\Phi(T)$ dependence in the fluctuation regime with theoretical predictions requires a better knowledge of the resistive mechanisms in this temperature regime, especially in the presence of a magnetic field.

C. $T_{c0}(B) < T < T_{c0}(B=0)$

Focusing on the temperature range with an approximately linear temperature dependence of $U_\Phi(T)$, we obtain $dU_\Phi/dT(B=3T)=-2.4\times10^{-15}$ J/K m. This is about 100 times smaller than the value of the epitaxial film. Because of the 90% a-axis orientation of the film, the external magnetic field is preferentially parallel to the a axis. The cores of the flux lines are centered between the CuO_2 planes, where the order parameter is smaller than in the CuO_2 planes. Thus the transport entropy is expected to be smaller than for $\mathbf{B}\|c$. Calculating the quantity $U_\Phi(T)$ for $\mathbf{B}\|\mathbf{a}$ and $\mathbf{B}\|\mathbf{c}$ according to Eqs. (4) and (5) with the values of κ_{GL} and dH_{c2}/dT reported in Ref. 19, the value of dU_Φ/dT for $\mathbf{B}\|\mathbf{a}$ was found to be lower by a factor of 8 than for $\mathbf{B}\|\mathbf{c}$.

In order to clarify the remaining discrepancy between the theoretical prediction and experimental data, we have measured the magnetic-field dependence of the resistivity and Nernst coefficient at a constant temperature $T < T_{c0}(B=0)$. For the correct interpretation of these data, it is instructive to compare these data with the corresponding data of the epitaxial film. In Fig. 6(a),

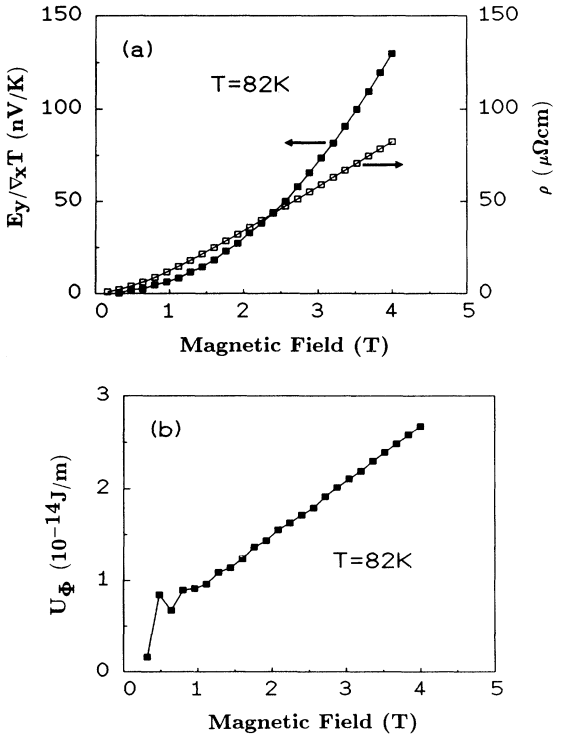

FIG. 6. Polycrystalline film. (a) Magnetic-field dependence of the Nernst coefficient and resistivity of strip A at $T=82$ K, (b) Magnetic-field dependence of the transport energy per unit length U_Φ calculated from the data shown in (a) using Eqs. (3) and (5).

$\rho(B,T=82\ \mathrm{K})$ and $E_y/\nabla_x T(B,T=82\ \mathrm{K})$ of the polycrystalline film are plotted. Figure 6(b) shows $U_\Phi(B,T=82\ \mathrm{K})$ calculated from these data using Eqs. (3) and (5). The data points were measured in the stationary state. For comparison, Fig. 7(a) shows the magnetic-field dependence of the resistivity and Nernst coefficient of the epitaxial film at $T=85$ K. The transport energy $U_\Phi(B)$ obtained from these data is shown in Fig. 7(b).

As shown in Fig. 6(b), $U_\Phi(B)$ of the polycrystalline film increases about linearly with increasing magnetic field. However, $U_\Phi(B)$ is expected to decrease with increasing field. The reason for this unexpected behavior becomes clear by comparing the $\rho(B)$ and $E_y/\nabla_x T(B)$ data of the polycrystalline and epitaxial samples.

The behavior of the epitaxial film can be understood as follows: Within a flux-creep model, the resistivity of the epitaxial film at a constant temperature follows the proportionality

$$\rho(B)\sim B\rho_0 \exp[-U(B)/k_B T]\ , \tag{12}$$

where $U(B)$ is the magnetic-field-dependent activation energy. Equation (12) explains the rapid increase of $\rho(B)$ for $B\leq 2$ T, as shown in Fig. 7(a). At larger fields the transition to the flux-flow regime occurs, which results in the observed nearly linear behavior of $U_\Phi(B)$ for $2<B<3$ T. Since at $T=85$ K, the upper critical field of the epitaxial film is about 8 T, the applied field only varies in the range $0\leq H\leq H_{c2}/2$, resulting in only a small decrease of U_Φ, as seen in Fig. 7(b). Consequently, a similar curvature is observed for $E_y/\nabla_x T(B)$ and for $\rho(B)$ [Fig. 7(a)], reflecting the behavior of epitaxial material due to the motion of Abrikosov vortices.

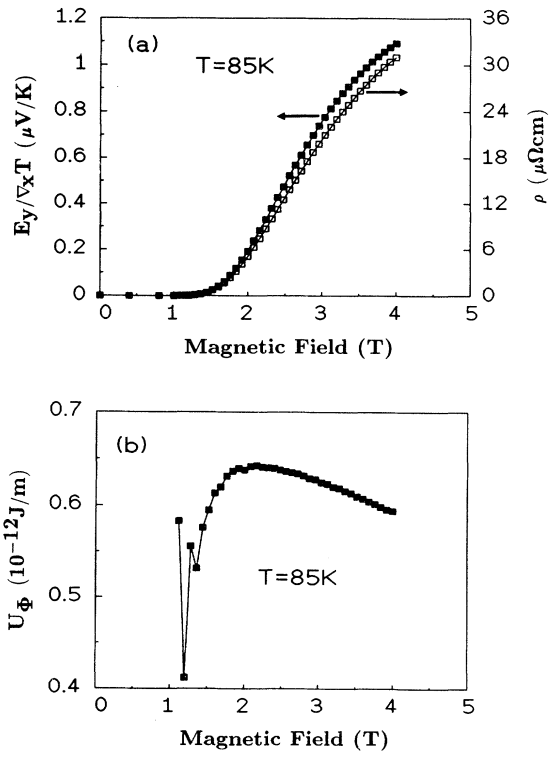

FIG. 7. Epitaxial film, (a) Magnetic-field dependence of the Nernst coefficient and resistivity of strip A at $T=85$ K. (b) Magnetic-field dependence of the transport energy per unit length U_Φ calculated from the data shown in (a) using Eqs. (3) and (5).

For the polycrystalline film we have $\mathbf{B}\perp\mathbf{c}$ due to the 90% a-axis orientation of the grains. At $T=82$ K, $H_{c2}>8$ T, and hence the flux-creep regime extends up to higher B values than in the case of the epitaxial film. The expected upward curvature of the $(E_y/\nabla_x T)(B)$ characteristic is indeed observed in Fig. 6(a). However, in contrast to the epitaxial film, the resistivity rises almost linearly with increasing magnetic field. Obviously, the resistivity of the polycrystalline film is composed of at least two contributions. The first, $\rho_{\mathrm{FF}}(B)$, is associated with the motion of Abrikosov vortices in the grains and should show a similar exponential form as the $E_y/\nabla_x T$ curve.

The second, which is the dominating part of the measured resistivity $\rho(B)$, is caused by a resistive mechanism not involving the motion of Abrikosov vortices. Consequently, according to the arguments outlined in Sec. II, $U_\Phi(B,T)$ calculated from the measured data is too small. Furthermore, an increasing ratio $\rho_{\mathrm{FF}}(B)/\rho_{\mathrm{GB}}(B)$ with increasing field results in an increasing function $U_\Phi(B)$, as shown in Fig. 6(b).

Summing up, we note that the calculation of U_Φ from the measured data of ρ and $E_y/\nabla_x T$ is very sensitive to the presence of additional resistive mechanisms not involving the motion of Abrikosov vortices as, for example, due to grain boundaries. The correct value of U_Φ is obtained only in the case of epitaxial material, where $\rho_{\mathrm{FF}}(B,T)=\rho(B,T)$ for $T<T_{c0}(B=0)$. Moreover, it is surprising that also in the polycrystalline film U_Φ increases linearly with decreasing temperature down to $T=T_{c0}(B)$, where the value of U_Φ is dominated by noise due to the small values of both ρ and $E_y/\nabla_x T$. That means that at least part of the resistivity is caused by moving Abrikosov vortices down to $T\approx T_{c0}(B)\approx 77$ K, whereas in epitaxial material without grain boundaries those vortices appear already completely pinned at the corresponding value of $T_{c0}(B)$.

D. T near $T_{c0}(B)$

Figure 5(c) shows that $U_\Phi(T)$ tends to decrease with decreasing temperature for $T\approx T_{c0}(B)$. This is confirmed by the single data point at 77.1 K marked by the arrow, which is taken from Fig. 3 and known with high accuracy. The same feature was observed for the epitaxial film [Fig. 4(c)], where also dU_Φ/dT changes sign at T near $T_{c0}(B)$. We have confirmed that this behavior is not caused by errors in the temperature, Nernst voltage, and resistivity data. A similar downward bending of $U_\Phi(T)$ is shown in Ref. 17, where the experimental data of Palstra *et al.*[15] are plotted down to lower temperatures. The observed curvature of $U_\Phi(T)$ close to $T_c(B)$ seems to be independent of the sample properties and, in particular, of the degree of inhomogeneity and experimental technique.

A possible explanation for this observation may be given within the Kosterlitz-Thouless (KT) model. Recently, Jensen and Minnhagen[10] have argued that the KT behavior established in high-T_c materials also should play a role in the presence of an external magnetic field. In particular, they have derived a relation between the applied field and KT transition temperature T_{KT}, which was shown to be in agreement with the experimental results published by Koch *et al.*[6]

Thus, if vortex-antivortex unbinding contributes to the measured resistivity, $U_\Phi(T)$ will be reduced, as outlined in Sec. II. Above T_{KT} the density of vortex pairs decreases rapidly with increasing temperature, since the increasing density of free vortices reduces their correlation length ξ_+, which determines the range of the logarithmic pair interaction above T_{KT}. Therefore, the additional resistivity $\rho_{KT}(T)$ due to the unbinding of vortex-antivortex pairs should decrease rapidly with increasing temperature. This would qualitatively explain the observed curvature in the $U_\Phi(T)$ data.

VI. CONCLUSION

We have developed a method, using the sample configuration itself for thermometry, to measure the characteristic of the Nernst electric field $E_y(\nabla_x T)$, keeping the temperature of the specimen at a constant value with high accuracy. Applying this technique, the temperature and magnetic-field dependences of the Nernst voltage has been investigated both in *c*-axis-oriented, epitaxial, and preferentially *a*-axis-oriented polycrystalline films of $YBa_2Cu_3O_{7-\delta}$. From the epitaxial film data, we obtain the value $-dH_{c2}/dT=2\pm0.5$ T K near T_c, resulting in a value for the coherence length, $\xi_{ab}(0)$, of about 17 Å and a value for κ_{GL} of 80 ± 10. We have shown that the determination of the transport entropy from the measured data of $E_y/\nabla_x T$ and ρ is very sensitive to the presence of additional resistive processes in the film not involving the motion of Abrikosov vortices. In particular, the correct value of the transport entropy per unit length of a single flux line can be obtained only for high quality epitaxial films or single crystals. The predominantly *a*-axis-oriented polycrystalline sample yield values for the derivative dU_Φ/dT about 100 times smaller than for the *c*-axis-oriented epitaxial film. This can be explained only partly by the anisotropy of $Y_1Ba_2Cu_3O_{7-\delta}$.

ACKNOWLEDGMENT

Financial support of this work by the Bundesminister für Forschung und Technologie (Project No. 13N5482) is gratefully acknowledged. We also would like to thank K. Knorr for performing the x-ray analysis of the *a*-axis-oriented polycrystalline films.

[1]Y. Yeshurun and A. P. Malozemoff, Phys. Rev. Lett. **60**, 2202 (1988).
[2]T. T. M. Palstra, B. Batlogg, R. B. van Dover, L. F. Schneemeyer, and J. V. Wasczak, Phys. Rev. B **41**, 6621 (1990); T. T. M. Palstra, B. Batlogg, L. F. Schneemeyer, and J. V. Waszczak, Phys. Rev. Lett. **61**, 1662 (1988).
[3]P. H. Kes, J. Aarts, J. van den Berg, C. J. van der Beek, and J. A. Mydosh, Supercond. Sci. Technol. **1**, 242 (1989).
[4]M. V. Feigel'man, V. B. Geshkenbein, A. I. Larkin, and V. Vinokur, Phys. Rev. Lett. **63**, 2303 (1989).
[5]R. Griessen, Phys. Rev. Lett. **64**, 1674 (1990).
[6]R. Koch, V. Foglietti, W. J. Gallagher, G. Koren, A. Gupta, and M. P. A. Fisher, Phys. Rev. Lett. **63**, 1511 (1989).
[7]M. P. A. Fisher, Phys. Rev. Lett. **62**, 1415 (1989).
[8]J. M. Kosterlitz and D. J. Thouless, J. Phys. C **6**, 1181 (1973).
[9]A. M. Kadin, K. Epstein, and A. M. Goldmann, Phys. Rev. B **27**, 6691 (1973).
[10]H. J. Jensen and P. Minnhagen, Phys. Rev. Lett. **66**, 1630 (1991).
[11]M. Zeh, H.-C. Ri, F. Kober, R. P. Huebener, J. Fisher, R. Gross, H. Mueller, T. Sermet, A. V. Ustinov, H.-G. Wener, and J. Mannhart, Physica C **167**, 6 (1990).
[12]M. Zeh, H.-C. Ri, F. Kober, R. P. Huebener, A. V. Ustinov, J. Mannhart, R. Gross, and A. Gupta, Phys. Rev. Lett. **64**, 3195 (1990).
[13]M. Galffy, A. Freimuth, and U. Murek, Phys. Rev. B **41**, 11 029 (1990).
[14]H. Lengfellner, A. Schnellbögl, J. Betz, W. Prettl, and K. F. Renk, Phys. Rev. B **42**, 6264 (1990).
[15]T. T. M. Palstra, B. Batlogg, L. F. Schneemeyer, and J. V. Waszczak, Phys. Rev. Lett. **64**, 3090 (1990).
[16]N. R. Werthamer, E. Helfand, and P. C. Hohenberg, Phys. Rev. **147**, 295 (1966).
[17]S. Ullah and A. T. Dorsey, Phys. Rev. Lett. **65**, 2066 (1990).
[18]S. J. Hagen, C. J. Lobb, R. L. Greene, M. G. Forrester, and J. Talvacchio, Phys. Rev. B **42**, 6777 (1990).
[19]U. Welp, W. K. Kwok, G. W. Crabtree, K. G. Vandervoort, and J. Z. Liu, Phys. Rev. Lett. **62**, 1908 (1990).
[20]Z. Hao, J. R. Clem, M. W. McElfresh, L. Civale, A. P. Malozemoff, and F. Holtzberg, Phys. Rev. B **43**, 2844 (1991).
[21]R. P. Huebener, *Magnetic Flux Structures in Superconductors* (Springer-Verlag, Berlin, 1979).
[22]K. Maki, J. Low Temp. Phys. **1**, 45 (1969).
[23]C.-R. Hu, Phys. Rev. B **13**, 4780 (1976).
[24]H.-C. Ri, F. Kober, R. Gross, R. P. Huebener, and A. Gupta, Phys. Rev. B **43**, 13739 (1991).
[25]D. Dijkkamp, T. Venkatesan, X. D. Wu, S. A. Shaheen, N. Jisrawi, Y. H. Min Lee, W. L. McLean, and M. Croft, Appl. Phys. Lett. **51**, 619 (1987).
[26]B. Roas, L. Schultz,, and G. Endres, Appl. Phys. Lett. **53**, 1557 (1988).
[27]G. Koren, A. Gupta, and R. J. Baseman, Appl. Phys. Lett. **54**, 1920 (1989).
[28]D. Koelle, F. Kober, M. Hartmann, R. Gross, R. P. Huebener, B. Roas, L. Schultz, and G. Saemann-Ischenko, Physica C **167**, 79 (1990).